Batteries & Supercaps

Research Article
doi.org/10.1002/batt.202300129

Chemistry Europe
European Chemical Societies Publishing

www.batteries-supercaps.org

The Use of Reductive Agents for Developing Capacity Balanced Aqueous Sodium-Ion Batteries

Milda Petrulevičienė,[a] Nadežda Traškina,[a] Jurgis Pilipavičius,[a, b] Jurga Juodkazytė,[a] and Linas Vilčiauskas*[a]

Aqueous sodium-ion batteries (Na-ion batteries) represent an attractive low cost stationary energy storage technology. However, limited electrochemical stability of water and issues related to complex aqueous chemistry, component corrosion, and materials dissolution limit their lifetime. Oxygen reduction reaction is considered to be the main parasitic process in aqueous Na-ion batteries leading to self-discharge, materials degradation and Na-ion inventory loss. Herein, we present a comprehensive study on novel electrolyte design which allows to mitigate the main parasitic reactions and prepare capacity balanced (N/P = 1) aqueous battery cells. For this purpose, aqueous symmetric $Na_2VTi(PO_4)_3$ | $Na_2VTi(PO_4)_3$ system is used as a model to demonstrate that the introduction of a small concentration of strongly reducing agent such as hydrazine into purely aqueous or hybrid (water and dimethyl sulphoxide) electrolyte could chemically reduce the dissolved oxygen and significantly improve the capacity retention of N/P = 1 cells during cycling. The low concentrations and self-consuming nature of hydrazine in a closed cell do not pose any health or chemical risks and presents a viable strategy for practical design. We believe, these results to be applicable not only to aqueous Na-ion batteries but also other aqueous or hybrid battery chemistries where such parasitic processes play a significant role.

Introduction

Aqueous ion insertion batteries represent an attractive alternative electrochemical energy storage technology due to their inherent safety, low environmental footprint, affordability, and scalability.[1] Generally, the limited electrolytic stability of aqueous electrolyte solutions results in reduced energy density restricting the application of such batteries to stationary applications.[2] A number of aqueous battery concepts based on different charge carrying ions, electrode/electrolyte chemistries and states or matter are under intense research and technological development.[1,2] Among them, aqueous sodium ion batteries (ASIB) are deemed to be very attractive for low cost stationary energy storage applications.[3] In order to have a competitive advantage, ASIBs must be based on simple salt (sulfate, nitrate, perchlorate, etc.) low concentration aqueous electrolyte solutions and relatively abundant electrode materials.[4] In addition to the narrow electrochemical stability window of water, there are also other issues related to complex aqueous chemistry, component corrosion, materials dissolution, etc. which limit the lifetime and commercial prospects of ASIBs.[1]

NASICON (Na Superlonic CONductor) phosphate framework compounds are among the most studied electrode materials for aqueous and non-aqueous Na-ion batteries.[5–8] They show high thermal and electrochemical stability, fast ionic conductivity and provide ability to tune the electrode potential by selecting appropriate transition metals.[5] Due to the favorable potential of the Ti^{III}/Ti^{IV} couple (~2.1 V vs. Na^+/Na) which is close to the hydrogen evolution reaction (HER) potential at neutral pH, NASICON-structured $NaTi_2(PO_4)_3$ (NTP) is probably the most studied and characterized ASIB negative electrode material.[9,10] On the opposite side, it is the V^{III}/V^{IV} redox couple corresponding to ~3.4 V vs. Na^+/Na in NASICON structure which is among the most studied.[9] Although a purely V-based NASICON $Na_3V_2(PO_4)_3$ (NVP) is a stable and widely used positive electrode material in non-aqueous Na-ion batteries, it is very unstable in aqueous electrolytes.[10,11] This is most likely due to the aqueous solubility and stability of $V^{(V)}$ species which inevitably form during electrochemical cycling.[11,12] It is also known that a partial substitution of vanadium by titanium substantially increases the electrochemical stability of NVP in simple aqueous electrolytes.[11,13–17] A range of $Na_{3-x}V_{2-x}Ti_x(PO_4)_3$ (NVTP) solid solution compositions show improved cycling stability in aqueous electrolytes.[11] This was attributed to some subtle effects in chemical bonding due to the introduction of Ti into the NASICON structure which tend to stabilize the V–O bonds.[11]

Interestingly, due to the presence of two, well separated redox pairs within the electrochemical window of water, NVTP can serve as a valuable model material for symmetric ASIBs. Although, symmetric batteries are not that useful for practical purposes *per se*, they are excellent model systems for studying materials electrochemical degradation, cell impedance spectra, mechanical properties, or electrode capacity balancing in full cells. The latter is a very important aspect of battery cell design

[a] Dr. M. Petrulevičienė, N. Traškina, Dr. J. Pilipavičius, Dr. J. Juodkazytė, Dr. L. Vilčiauskas
Center for Physical Sciences and Technology (FTMC)
Saulėtekio al. 3, LT-10257, Vilnius (Lithuania)
E-mail: linas.vilciauskas@ftmc.lt
[b] Dr. J. Pilipavičius
Institute of Chemistry, Vilnius University
Naugarduko 24, LT-03225, Vilnius (Lithuania)

Research Article
doi.org/10.1002/batt.202300129
Chemistry Europe
European Chemical Societies Publishing

and engineering and has significant consequences not only for the overcapacity requirements for the electrodes but also cell cycling lifetime and self-discharge characteristics.[11,18,19] Our previous study of full NVTP|NVTP cells clearly indicated that it is not the capacity loss of individual electrodes but rather that of a charge carrying ion inventory, which is responsible for electrode capacity imbalance leading to cell capacity decay.[11] Various parasitic reactions are usually responsible for this loss. In the case of Li-ion batteries, it is typically the formation of Li-rich solid-electrolyte interphase, whereas in ASIBs it is usually the hydrogen evolution reaction (HER), oxygen evolution reaction (OER), or oxygen reduction reaction (ORR). ORR was previously identified as the main parasitic process leading to alkalization at the negative NTP electrode interface and its subsequent degradation.[11,20,21] Although most of the dissolved oxygen reduction takes place during the several initial cycles in a closed system, the effects of this process tend to propagate to later cycles.[11] The mitigation of parasitic reactions such as ORR is key for making ASIBs with sufficient cycling stability. One way to mitigate this problem is a design overcapacity of the cathode.[22,23] However this introduces deadweight into the system and results in higher materials and manufacturing bills. Therefore, a possibility to design and prepare capacity balanced cells, i.e., those with equal negative and positive electrode capacity or N/P = 1 cells is highly desired.

In the present work, we show that a careful design and optimization of aqueous electrolytes could mitigate the most critical parasitic reactions in NVTP|NVTP ASIBs. The introduction of a very small concentration around 0.1 mol% of strongly reducing agent such as hydrazine into the aqueous or hybrid (e.g., water and dimethyl sulphoxide (DMSO)) electrolyte solutions chemically reduces the dissolved oxygen and significantly improves the capacity retention of N/P = 1 NVTP|NVTP cells. The low concentration and self-consuming nature of hydrazine in closed cells do not pose any health or chemical risks and is a viable practical strategy for practical purposes. We believe these results to be also applicable and useful in other aqueous battery chemistries where such or similar parasitic processes play a significant role.

Results and Discussion

Half-cell characterization of NVTP electrodes

In our previous study of the $Na_{3-x}V_{2-x}Ti_x(PO_4)_3$ ($0 < x < 1$) system, a detailed analysis of the vanadium redox processes and the influence of titanium substitution on their stability was presented.[11] In this study, both the vanadium and titanium electrochemical redox processes in $Na_2VTi(PO_4)_3$ are fully characterized. The cyclic voltammogram of a NVTP electrode recorded in 1 M Na_2SO_4 (aq.) in the range of potentials encompassing both Ti and V redox reactions is shown in Figure 1(a). Two pairs of reversible peaks centered at ca. −1.2 V and 0 V (vs. Hg/Hg_2SO_4) correspond to Ti^{III}/Ti^{IV} and V^{III}/V^{IV} redox transitions accompanied by de-/insertion of sodium ions:

$$Na_2V^{III}Ti^{IV}(PO_4)_3 + e^- + Na^+ \leftrightarrow Na_3V^{III}Ti^{III}(PO_4)_3 \quad (1)$$

$$Na_2V^{III}Ti^{IV}(PO_4)_3 - e^- - Na^+ \leftrightarrow NaV^{IV}Ti^{IV}(PO_4)_3 \quad (2)$$

The galvanostatic charge/discharge (GCD) cycling stability of NVTP is tested by cycling the electrodes in the appropriate potential range of Ti^{III}/Ti^{IV} and V^{III}/V^{IV} redox processes at 1 C rate. The Coulombic efficiency (CE) and specific charge capacity for 100 GCD cycles is shown in Figures 1(b) and (c), respectively. CE for the vanadium side reaches almost 100% after the first 5 cycles and remains stable during experiment (Figure 1c). The situation is different for the titanium side, the CE only reaches between 85% and 90% and shows significant fluctuations throughout cycling. The capacity retention of NVTP is 96% and about 80% as a negative and a positive electrode, respectively. The observed behavior indicates the presence of additional parasitic reactions especially prominent on the negative side. Oxygen reduction reaction (ORR) was identified as the dom-

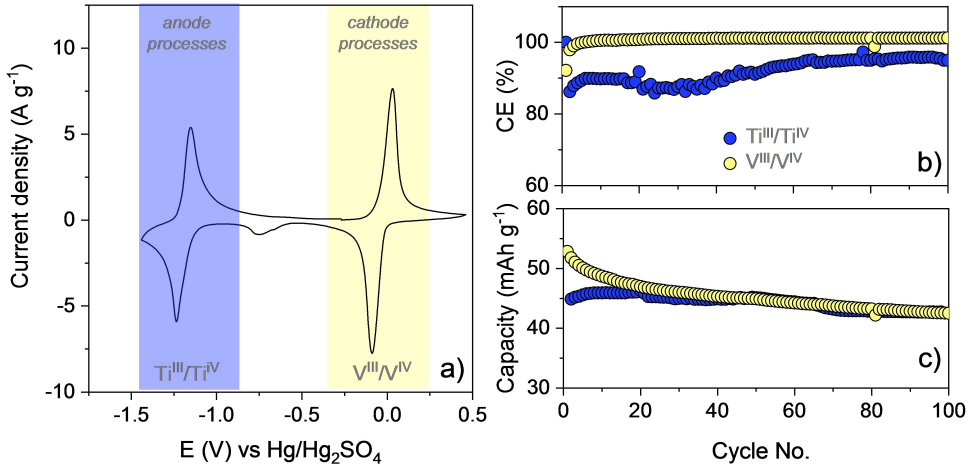

Figure 1. a) Cyclic voltammogram of a NVTP electrode in 1 M Na_2SO_4 (aq.) recorded at 5 mV s^{-1}; b) Coulombic efficiency and c) specific discharge capacity for Ti and V redox process in NVTP electrodes during GCD cycling at 1 C rate.

Research Article
doi.org/10.1002/batt.202300129
Chemistry Europe
European Chemical Societies Publishing

inant parasitic process during the electrochemical cycling of $NaTi_2(PO_4)_3$ and $Na_2VTi(PO_4)_3$ anodes. Ti^{III}-catalyzed ORR causes self-discharge and leads to local pH changes leading to anode degradation especially at slow ($\leq$1 C) GCD rates.[11,21] The redox behavior of carbonaceous phase which is typically present in substantial quantities in battery electrode composites is among other side reactions taking place on aqueous electrodes.[24] These processes are typically irreversible and visible as a smaller cathodic peak at ca. −0.74 V vs. Hg/Hg_2SO_4 in the first CV cycle in Figure 1(a).

Full cells

Hydrazine (N_2H_4) is a well-known oxygen scavenger widely used in industry to avoid corrosion.[25] Although designated as hazardous and carcinogenic material, it is relatively safe at low concentrations as an aqueous solution, and is actually self-consumed when used in a closed system.[26] In this study, hydrazine as a strongly reductive agent is employed for solving two issues related to aqueous ion batteries at the same time. First, in aqueous solutions it reacts with dissolved oxygen to yield nitrogen and water:

$$N_2H_4 + O_2 \rightarrow N_2 + 2H_2O \quad (3)$$

Second, hydrazine is a widely used reducing agent to prepare carbon materials such as reduced graphene oxide.[27] It acts as a reducing agent on the carbonyl functional groups present on the surface of carbon via Wolff-Kishner type reduction:

$$\begin{aligned} &> C{=}O\ (\text{surface}) + N_2H_4 \\ &\leftrightarrow > CH_2\ (\text{surface}) + N_2 + H_2O \end{aligned} \quad (4)$$

or epoxide groups on the surface of carbon via Wharton type reaction:

$$\begin{aligned} &> C{-}O{-}C <\ (\text{surface}) + N_2H_4 \\ &\leftrightarrow -CH{=}CH-\ (\text{surface}) + N_2 + H_2O \end{aligned} \quad (5)$$

This property helps to save the active ion inventory and leads to better electrode capacity balance in the cycling of ASIBs.

In order to evaluate the effect of N_2H_4 on the electrode processes in symmetric NVTP full cells a set of experiments were performed in 3-electrode T-type cells. The employed electrolyte is 1 M Na_2SO_4 (aq.) containing different amounts of hydrazine: 0, 0.01, 0.02, 0.1, 0.15 mol%. The recorded potential profiles for the first charging cycle of the negative and positive electrodes are shown in Figure 2. The results indicate that increasing N_2H_4 concentration has a threefold effect: 1) the open circuit potential (OCP) shifts to more negative values with increasing N_2H_4 concentration, 2) the feature at ca. −0.6 V vs. Hg/Hg_2SO_4 corresponding to the reduction of carbonaceous phase disappears when $c(N_2H_4)$ exceeds 0.01 mol%, and the anode potential reaches the plateau faster at higher $c(N_2H_4)$, 3)

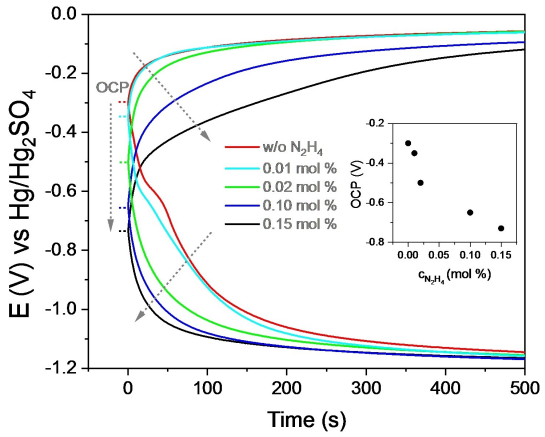

Figure 2. Charging profiles for anode and cathode in symmetric NVTP full cells in the first cycle recorded in 1 M Na_2SO_4 (aq.) at 1 C rate and different hydrazine concentration. The inset in the graph depicts the dependence of open circuit potential on $c(N_2H_4)$.

the trend for cathode potential is opposite – higher $c(N_2H_4)$ leads to longer times to reach the potential plateau. The first two results are interrelated because N_2H_4 present in the electrolyte chemically reduces the carbon surface and leads to negative shift in OCP value. On the other hand, the variation of cathode potential with respect to $c(N_2H_4)$ can be related to the electrooxidation of hydrazine itself. It has been recently demonstrated that hydrazine molecules are electroactive only in their unprotonated form i.e., N_2H_4, whereas the protonated species $N_2H_5^+$ are electrochemically inactive with pK_a of 8.2.[28] This also indicates that in near neutral 1 M Na_2SO_4 (aq.), some portion of dissolved hydrazine can undergo an electrooxidation reaction according to:

$$N_2H_4 - 4e^- \rightarrow N_2 + 4H^+ \quad (6)$$

The latter process increases the electrolyte acidity and also leads to protonation of hydrazine, making Reaction 6 self-inhibiting. This suggests that excessive amount of hydrazine in electrolyte solution might result in unfavorable equilibrium which is not beneficial for the electrochemistry of NVTP|NVTP cells. The results presented in Figure 2 indicate that in this system ca. $c(N_2H_4) = 0.1$ mol% is an optimal concentration and was chosen for further experiments in this work. Another important aspect to consider is that chemical reducing ability of N_2H_4 is much higher than that of its protonated form, $N_2H_5^+$, as can be judged from the values of standard potentials.[29]

$$\begin{aligned} &N_2H_5^+ - 4e^- \rightarrow N_2 + 5H^+ \\ &E^0 = -0.22\ \text{V (vs. SHE)} \end{aligned} \quad (7)$$

$$N_2H_4 + 4OH^- - 4e^- \rightarrow N_2 + 4H_2O\ E^0 = -1.17\ \text{V (vs. SHE)} \quad (8)$$

This is the reason why aqueous hydrazine solutions are unstable under alkaline or neutral conditions but quite stable under strongly acidic conditions.[30] Therefore, a careful pH adjustment and control also play a significant role in hydrazine

Research Article
doi.org/10.1002/batt.202300129
Chemistry Europe
European Chemical Societies Publishing

electrochemistry. It is important to note that for other systems, the optimum hydrazine concentration should be carefully tuned and will strongly depend on the oxygen solubility and acid-base equilibrium in a particular electrolyte.

A set of GCD cycling experiments were performed in 2-electrode symmetric NVTP|NVTP full cells with different electrolyte compositions while keeping the electrode capacity ratio at 1 (N/P = 1) (see Table 1 for the nomenclature of electrolytes). In Figure 3(a) the GCD cycling performance of cells with S_7 and S_7_HZ electrolytes is compared. In the absence of N_2H_4 (S_7 electrolyte), the capacity of the cell drops from 35 to 15 mAh g^{-1} during the first 10 cycles. As demonstrated in our previous study,[11] such decrease in cell capacity is related to fast capacity disbalance, because there is no excess of capacity in cathode to compensate for charge consumed by parasitic ORR at the anode. This is corroborated by low values of CE, which ranged from ~60 to ~80% in the first 10 cycles. The discharge capacity retention after 100 GCD cycles was less than 25%. The addition of 0.1 mol% of N_2H_4 (S_7_HZ), results in much slower capacity fade and doubling of capacity retention (~53%). The observed increase in CE is much steeper which supports the suppression of parasitic processes in the cell. The charge/discharge profiles for the first cycles in S_7 and S_7_HZ are shown in Figure 3(d). These profiles in both electrolytes almost coincide within the voltage range from 0 to 1 V, suggesting that either all of hydrazine was consumed in the reaction with O_2, or it stays in electrochemically inactive $N_2H_5^+$ form. A slight divergence of the curves in the beginning of the charging should be attributed to the electroreduction of carbonaceous species in S_7 electrolyte, while in the case of S_7_HZ this process is not visible because of chemical reduction of carbon surface by N_2H_4.

Interestingly, the addition of 0.1 M sodium borate buffer to fix the pH at 10 in 1 M Na_2SO_4 (aq.) led to even faster capacity decay of a symmetric NVTP|NVTP cell (Figure 3b) compared to unbuffered 1 M Na_2SO_4 (aq.) electrolyte (Figure 3a). The observed low values of CE (< 80%) point to strong influence of parasitic processes. This suggests that just raising the pH value does not stop the active ion inventory loss and still leads to fast capacity decay. However, the addition of 0.1 mol% N_2H_4 to this electrolyte (S_10_HZ) dramatically improves the capacity retention (78%) after 100 GCD cycles with CE being ~96% (Figure 3b). The charge/discharge profiles in Figure 3(e) demonstrate that electrochemical oxidation of N_2H_4 lowers the CE in the first cycle suggesting that at pH = 10, the majority of N_2H_4 is in the electrochemically active form and is oxidized in the first cycle because the charging capacity of the second cycle is significantly lower (Figure 3b).

In this work, a hybrid electrolyte containing 1 M $NaNO_3$ in DMSO/H_2O (N_DMSO) was also tested. Even though the oxygen solubility is typically higher in organic solvents, this hybrid electrolyte is known to have a significantly reduced relative

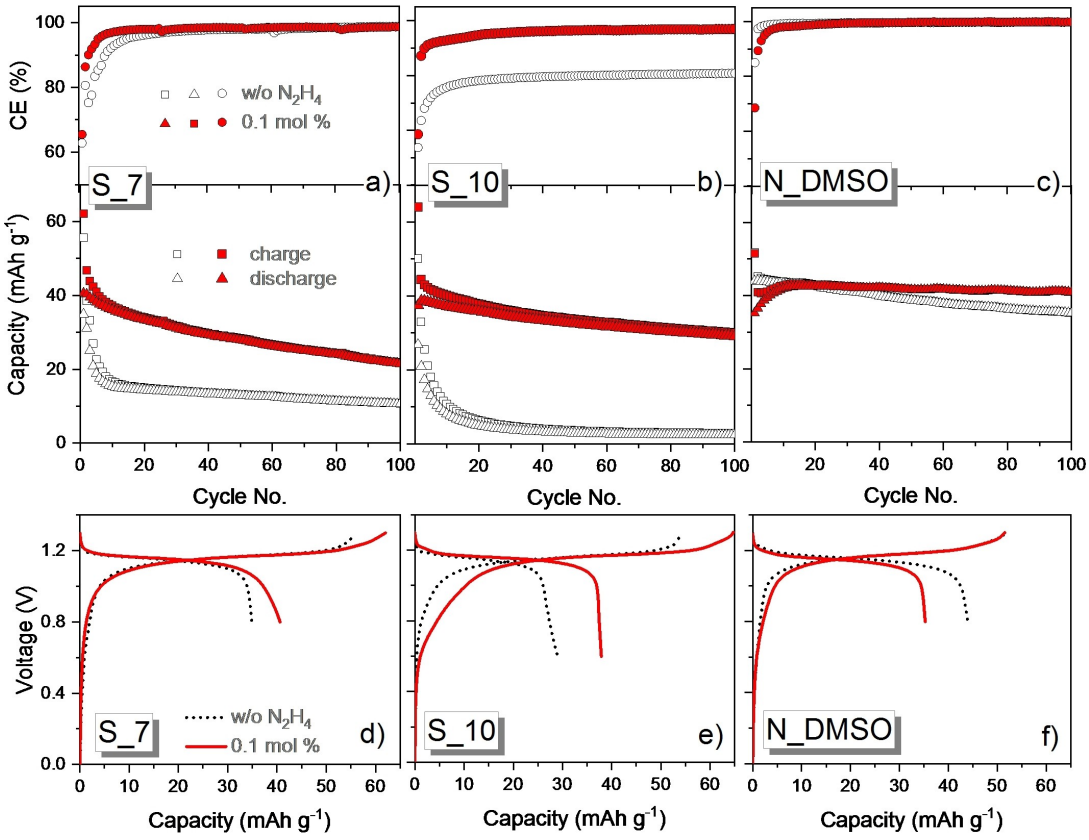

Figure 3. a–c) Variation of specific discharge capacity and Coulombic efficiency together with d–f) voltage-capacity profiles of the first cycle recorded during GCD cycling at 1 C rate of symmetric NVTP|NVTP cells with N/P = 1 in a,d) S_7 with and w/o 0.1 mol% N_2H_4, b,e) S_10 with and w/o 0.1 mol% N_2H_4, c,f) N_DMSO with and w/o 0.1 mol% N_2H_4 electrolyte solutions.

Research Article
doi.org/10.1002/batt.202300129
Chemistry Europe
European Chemical Societies Publishing

water activity which changes aqueous chemistry and affects the parasitic reactions. The GCD cycling results presented in Figure 3(c) show a significantly more stable cycling performance of NVTP|NVTP even in the absence of N_2H_4. The capacity retention after 100 cycles is as high as ~80% and the CE reaches almost 100% within the first 5 cycles. Nevertheless, the addition of 0.1 mol% N_2H_4 into the electrolyte (N_DMSO_HZ) leads to even further improvement in terms of capacity retention (Figure 3c). The electro-oxidation of hydrazine is visible in the charging profile of the first cycle (Figure 3f), however the equilibrium of N_2H_4 protonation reaction in N_DMSO_HZ electrolyte is probably very different from that of S_10_HZ. Although the CE values in the first couple of GCD cycles are relatively low and similar to those of fully aqueous systems, they stabilize within ~15 cycles. The results show that both CE and capacity retention stay at almost 100% during GCD cycling which is the best result for capacity balanced (N/P = 1) NVTP|NVTP cells obtained in this study.

In order to better understand the processes taking place at the anode and cathode, the potential profiles of individual electrodes were also recorded for multiple GCD cycles. In these experiments the total cell voltage was kept in the window between 0.6 and 1.3 V. Figure 4 shows the potential profiles corresponding to $Ti^{IV/III}$ and $V^{III/IV}$ redox reactions in different electrolytes. In hydrazine-free electrolytes, Ti^{IV} is reduced to Ti^{III} in the first charging cycle with the potential limited between −1 V and −1.21 V, whereas V^{III} is oxidized to V^{IV} in the potential range limited from −0.2 V to 0.1 V. Once one of the potential cut-offs is reached, the process is reversed to discharge phase and vice versa. As one can see, in the first charging cycle Ti is not completely reduced due to parasitic reactions (mainly ORR), which consume Na-ion inventory (Figure 4a). However, most of the V is almost fully oxidized and in the next cycle due to still occurring parasitic reactions Ti is again not completely reduced with V getting completely oxidized. Therefore, in every subsequent cycle less and less of Ti and V participate in electrochemical reactions leading to cell capacity fade. The addition of 0.1 mol% of hydrazine into the electrolyte solution changes the situation completely (Figure 4 (red line)). Ti is completely reduced in the first cycle and only in later cycles some previously described disbalance becomes visible. This is still probably due to the presence of some ORR or even HER taking place in the cell. In the alkaline 1 M Na_2SO_4 buffered electrolyte (pH ~10) without hydrazine the situation is similar to neutral 1 M Na_2SO_4 (Figure 4b). With the addition of hydrazine, a clear oxidation plateau of N_2H_4 is observed between −0.5 and −0.2 V vs. Hg/Hg_2SO_4 in the first charging cycle. This observation confirms that in alkaline solution hydrazine is electrochemically significantly more active resulting in much better capacity retention. Figure 4(c) shows the charge/discharge curves in 1 M $NaNO_3$ in DMSO/H_2O and 1 M $NaNO_3$ in DMSO/H_2O + 0.1% N_2H_4 solutions. One can see that in a system without hydrazine, both Ti and V are completely reduced and oxidized, respectively. However, this process slowly gets out of balance in later cycles. The addition of hydrazine seems to completely eliminate the parasitic reactions and charge/discharge profiles look almost identical during GCD cycling.

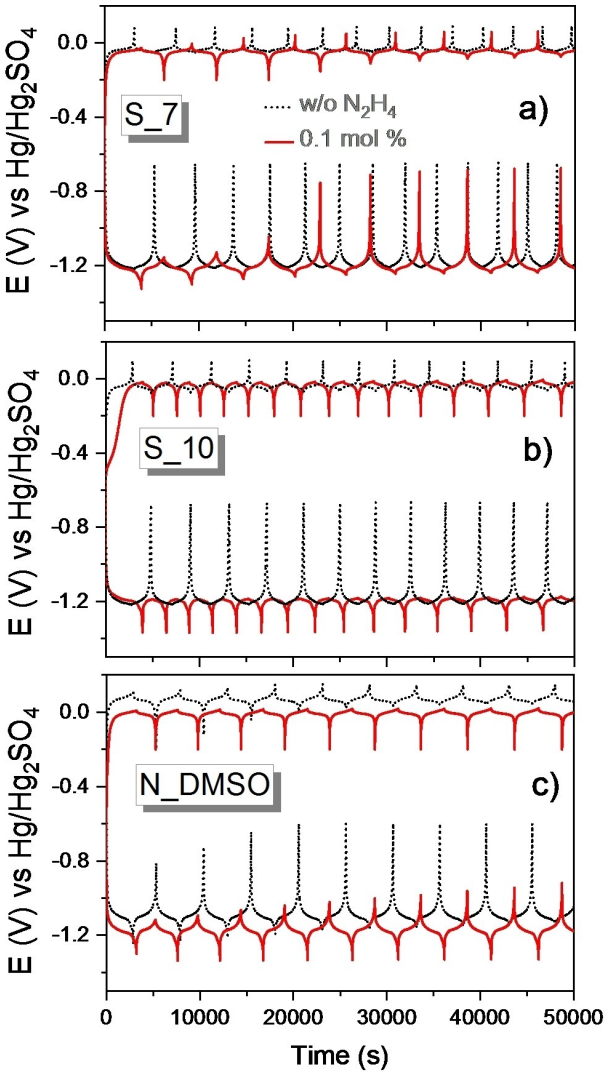

Figure 4. Anode and cathode potential *vs* time profiles of NVTP|NVTP symmetric cells measured in a) S_7 with and w/o 0.1 mol% N_2H_4, b) S_10 with and w/o 0.1 mol% N_2H_4, c) N_DMSO with and w/o 0.1 mol% N_2H_4 electrolytes. Black dotted line – electrolytes without N_2H_4, red solid line - electrolytes with 0.1 mol% of N_2H_4.

Investigations of self-discharge in full cells

As discussed in previous Sections, ORR is deemed to be the main parasitic process leading to low CE and causing self-discharge of NTP and NVTP electrodes in aqueous electrolytes.[11,21,31] The reaction between charged NVTP anode and dissolved oxygen can be written as:

$$4Na_3Ti^{III}V^{III}(PO_4)_3 + O_2 + 2H_2O \leftrightarrow 4Na_2Ti^{IV}V^{III}(PO_4)_3 + 4Na^+ + 4OH^- \quad (9)$$

The electrons from NVTP to O_2 are likely transferred via the conductive carbon present in the electrode composite. There-

Research Article
doi.org/10.1002/batt.202300129
Chemistry Europe
European Chemical Societies Publishing

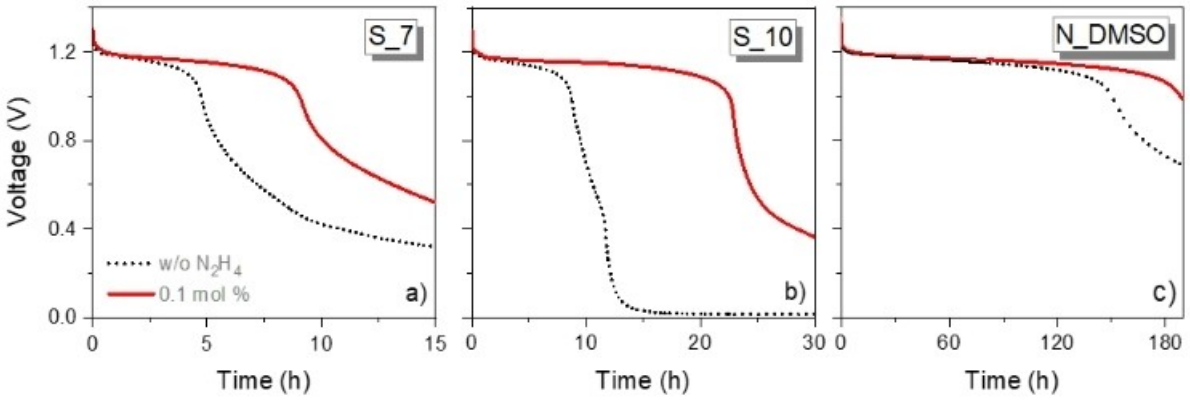

Figure 5. Self-discharge of symmetric NVTP | NVTP cells in a) S_7 with and w/o 0.1 mol % N_2H_4, b) S_10 with and w/o 0.1 mol % N_2H_4, c) N_DMSO with and w/o 0.1 mol % N_2H_4 electrolytes.

fore Reaction 9 can be divided into the following oxidation and reduction steps:

$$Na_2V^{III}Ti^{III}(PO_4)_3 - e^- \rightarrow NaV^{III}Ti^{IV}(PO_4)_3 + Na^+ \ (\text{vs. Reaction 2})$$

$$O_2 + 2H_2O + 4e^- \rightarrow 4OH^- \qquad (10)$$

It is noteworthy that the mechanism of ORR Reaction 9 is influenced by thermodynamic factors such as temperature, electrode potential, oxygen concentration, pH of the electrolyte etc., as well as kinetic factors which include the formation of reaction intermediates (e.g., H_2O_2), electrochemically active surface area and structure of the electrode that can affect the adsorption and desorption of reactive species. Furthermore, the ORR rate can also be influenced by composition, ionic conductivity and viscosity of the electrolyte.

The process of self-discharge in symmetric NVTP | NVTP batteries (N/P = 1) was investigated in 3-electrode T-type cells. The cells were assumed to be air-tight and no additional measures were taken to prevent the access of oxygen during the measurements. The electrolytes were kept under ambient conditions before assembling the cells. The cells were first charged at 1 C rate until the voltage reached 1.3 V and then kept under open circuit voltage (OCV) conditions in addition to monitoring this voltage over time. The results presented in Figure 5 show that the addition of 0.1 mol % N_2H_4 to S_7 electrolyte almost doubles the self-discharge time. The additional buffering of the electrolyte at pH = 10 doubles the self-discharge time even further and explains much slower capacity fade and higher capacity retention observed in GCD cycling. The cells with hybrid electrolyte did not self-discharge for ~155 h, indicating that decreasing relative water activity suppresses many aqueous parasitic processes. The addition of hydrazine extended the self-discharge time even further up to almost 200 h which also explains the GCD cycling performance of these cells. The comparative analysis of self-discharge time and capacity retention (data from Figure 3) versus electrolyte composition is presented in Figure 6. It is evident that in terms of capacity retention, addition of very small amount of N_2H_4 to aqueous 1 M Na_2SO_4 produces the same effect as mixing

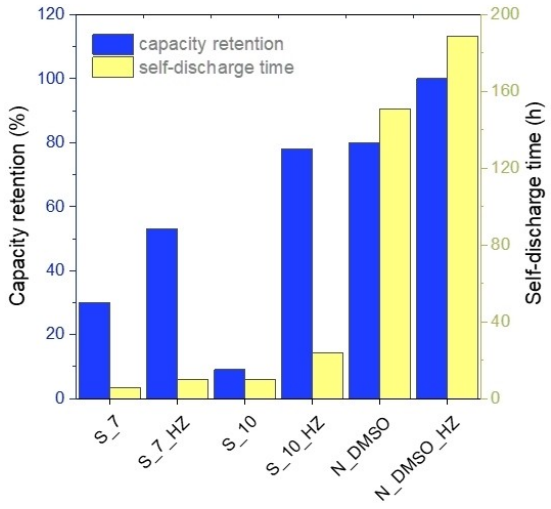

Figure 6. Capacity retention (%) and self-discharge time of NVTP | NVTP of coin and Swagelok-type cells, respectively with N/P = 1.

aqueous electrolyte solution with DMSO in 1:1 H_2O:DMSO molar ratio.

Conclusions

In this study, an aqueous symmetric $Na_2VTi(PO_4)_3$ | $Na_2VTi(PO_4)_3$ system is prepared and investigated as a model for electrolyte design and optimization with the aim of mitigating the main parasitic reactions in aqueous Na-ion batteries and making capacity balanced (N/P = 1) battery cells. Oxygen reduction reaction is known to be the main parasitic process leading to self-discharge, Na-ion inventory loss, and material degradation in aqueous Na-ion batteries. In this work, we demonstrate that the introduction of a small concentration (ca. 0.1 mol %) of strongly reducing agent such as hydrazine into the aqueous or hybrid (e.g., water and dimethyl sulphoxide (DMSO)) electrolyte solutions, chemically reduces the dissolved oxygen and significantly improves the capacity retention of N/P = 1 cells. Such low concentrations and the self-consuming nature of hydrazine

Research Article
doi.org/10.1002/batt.202300129
Chemistry Europe
European Chemical Societies Publishing

Table 1. The nomenclature of electrolytes used in this work. Abbreviations: S – sodium sulfate, N – sodium nitrate, SBB – sodium borate buffer, HZ – hydrazine.

Electrolyte composition and pH	Notation
1 M Na_2SO_4 (aq.) (pH = 7)	S_7
1 M Na_2SO_4 (aq.) + 0.1 mol % N_2H_4	S_7_HZ
1 M Na_2SO_4 (aq.) + 0.1 M SBB (pH = 10)	S_10
1 M Na_2SO_4 (aq.) + 0.1 M SBB + 0.1 mol % N_2H_4	S_10_HZ
1 M $NaNO_3$ in DMSO/H_2O	N_DMSO
1 M $NaNO_3$ in DMSO/H_2O + 0.1 mol % N_2H_4	N_DMSO_HZ

in closed cells do not pose any health or chemical risks and present a viable strategy for practical cell design and applications. Due to the absence of deadweight, N/P = 1 cells are highly desired by battery industry due to simpler design and lower materials and manufacturing costs. We believe these results to be applicable not only in the particular case of aqueous Na-ion batteries but also useful in other aqueous battery chemistries where such or similar parasitic processes might play a significant role.

Experimental Section

Preparation of materials and electrodes

$Na_2VTi(PO_4)_3$ electrodes were prepared from previously synthesized materials using identical procedures and protocols as described in our previous work.[11] For the preparation of electrolyte solutions, sodium sulfate (Na_2SO_4, 99.5 % Chempur), sodium nitrate ($NaNO_3$, ≥ 99.0 %, Acros organics), boric acid (H_3BO_3, 100 %, Reachem), sodium hydroxide (NaOH, 100 %, Standlab), dimethylsulfoxide ($(CH_3)_2SO$, 99.9 %, Reachem), and aqueous hydrazine solution (N_2H_4, 70 wt%, Reachem) were used. Six different electrolyte compositions were used in this study: 1 M Na_2SO_4 (aq.) (pH ~ 7), 1 M Na_2SO_4 (aq.) + 0.1 mol % N_2H_4 (pH ~ 10), 1 M Na_2SO_4 (aq.) + 0.1 M sodium borate buffer (pH = 10), 1 M Na_2SO_4 (aq.) + 0.1 M sodium borate buffer + 0.1 mol % N_2H_4; 5) 1 M $NaNO_3$ in DMSO/H_2O (molar ratio 1 : 1); 1 M $NaNO_3$ in DMSO/H_2O + 0.1 mol % N_2H_4. The DMSO : H_2O mixture at 1 : 1 molar ratio will be referred to as DMSO/H_2O throughout the text. The nomenclature of electrolytes used in this work is described in Table 1.

Half-cell electrochemical characterization

Electrochemical half-cell characterization of NVTP electrodes was performed in a bottom-mount beaker-type three-electrode cell for flat samples. Ag/AgCl/3 M KCl (aq.) and graphite rod were used as reference and counter electrodes, respectively. Cyclic voltammograms (CV) were recorded at 5 mV s^{-1} using a potentiostat/galvanostat (SP-240, Biologic). Galvanostatic charge-discharge (GCD) experiments were performed in potential ranges from 0.1 to 0.7 V vs. Ag/AgCl and from −1 to −0.6 vs. Ag/AgCl for positive vanadium and negative titanium electrode processes respectively. These experiments were carried out on a battery cycler (CT-4008, Neware). The specific current of 62.5 mA g^{-1} based on one-electron process theoretical specific capacity of NVTP was considered as 1 C rate in all experiments.

Full-cell electrochemical characterization

The symmetric NVTP | NVTP cells were assembled as CR2032 coin-type cells or as in-house machined three-electrode Swagelok-type T-cells. GF/D Rotilabo glass fiber separator (Carl Roth GmbH) was used in cell assembling. After cutting, the electrodes were purposely selected to have matching weights as there was a slight variation in terms of batch thickness. The variation in terms of capacity ratio for full cells was at most equal to several percent due to weighing error. The potentials of both positive and negative electrodes during GCD cycling were independently monitored with respect to a single $Hg/Hg_2SO_4/K_2SO_4$ (sat., aq.) reference electrode in the three-electrode T-cell experiments. The cell voltage window was set to 0.6–1.3 V in GCD cycling experiments. All potential values in the text are reported relative to $Hg/Hg_2SO_4/K_2SO_4$ (sat., aq.) (0.64 V vs. SHE) electrode unless noted otherwise.

Acknowledgements

This project has received funding from the European Regional Development Fund (Project No. 01.2.2-LMT-K-718-02-0005) under a grant agreement with the Research Council of Lithuania (LMTLT).

Conflict of Interests

L.V., J.J., J.P., M.P., N.T. have filed a patent application under No. 18/150,857 with the United States Patent and Trademark Office for the use of strongly reducing agents in aqueous ion insertion batteries.

Data Availability Statement

The data that support the findings of this study are available from the corresponding author upon reasonable request.

Keywords: aqueous sodium-ion batteries · symmetric batteries · NVTP · hydrazine · oxygen reduction

[1] D. Wu, X. Li, X. Liu, J. Yi, P. Acevedo-Peña, E. Reguera, K. Zhu, D. Bin, N. Melzack, R. G. A. Wills, J. Huang, X. Wang, X. Lin, D. Yu, J. Ma, *J. Phys. Energy* **2022**, *4*, 041501.
[2] D. Chao, W. Zhou, F. Xie, C. Ye, H. Li, M. Jaroniec, S.-Z. Qiao, *Sci. Adv.* **2020**, *6*, eaba4098.
[3] D. Bin, F. Wang, A. G. Tamirat, L. Suo, Y. Wang, C. Wang, Y. Xia, *Adv. Energy Mater.* **2018**, *8*, 1703008.
[4] H. Zhang, X. Liu, H. Li, I. Hasa, S. Passerini, *Angew. Chem. Int. Ed.* **2021**, *60*, 598.
[5] C. Masquelier, L. Croguennec, *Chem. Rev.* **2013**, *113*, 6552.
[6] Q. Zhang, C. Liao, T. Zhai, H. Li, *Electrochim. Acta* **2016**, *196*, 470.
[7] M. Sawicki, L. L. Shaw, *RSC Adv.* **2015**, *5*, 53129.
[8] C. Delmas, *Adv. Energy Mater.* **2018**, *8*, 1703137.
[9] K. Saravanan, C. W. Mason, A. Rudola, K. H. Wong, P. Balaya, *Adv. Energy Mater.* **2013**, *3*, 444.
[10] W. Song, X. Ji, Y. Zhu, H. Zhu, F. Li, J. Chen, F. Lu, Y. Yao, C. E. Banks, *ChemElectroChem* **2014**, *1*, 871.
[11] M. Petrulevičienė, J. Pilipavičius, J. Juodkazytė, D. Gryaznov, L. Vilčiauskas, *Electrochim. Acta* **2022**, *424*, 140580.

[12] E. Boivin, J.-N. Chotard, C. Masquelier, L. Croguennec, *Molecules* **2021**, *26*, 1428.
[13] C. W. Mason, F. Lange, *ECS Electrochem. Lett.* **2015**, *4*, A79.
[14] H. Zhang, S. Jeong, B. Qin, D. Vieira Carvalho, D. Buchholz, S. Passerini, *ChemSusChem* **2018**, *11*, 1382.
[15] L. Shen, H. Yang, Y. Jiang, J. Ma, T. Sun, M. Zhang, N. Zhu, *ACS Sustainable Chem. Eng.* **2021**, *9*, 3490.
[16] J. Dong, G. Zhang, X. Wang, S. Zhang, C. Deng, *J. Mater. Chem. A* **2017**, *5*, 18725.
[17] K. Nakamoto, R. Sakamoto, Y. Nishimura, J. Xia, M. Ito, S. Okada, *Electrochemistry* **2021**, *89*, 415.
[18] J. Kasnatscheew, T. Placke, B. Streipert, S. Rothermel, R. Wagner, P. Meister, I. C. Laskovic, M. Winter, *J. Electrochem. Soc.* **2017**, *164*, A2479.
[19] F. Reuter, A. Baasner, J. Pampel, M. Piwko, S. Dörfler, H. Althues, S. Kaskel, *J. Electrochem. Soc.* **2019**, *166*, A3265.
[20] A. I. Mohamed, J. F. Whitacre, *Electrochim. Acta* **2017**, *235*, 730.
[21] G. Plečkaitytė, M. Petrulevičienė, L. Staišiūnas, D. Tediashvili, J. Pilipavičius, J. Juodkazytė, L. Vilčiauskas, *J. Mater. Chem. A* **2021**, *9*, 12670.
[22] L. Yukun, L. Jie, S. Qiuyu, J. Zhang, H. Pingge, Q. Xuanhui, L. Yongchang, *eScience* **2022**, *2*, 10–31.
[23] J. F. Whitacre, S. Shanbhag, A. Mohamed, A. Polonsky, K. Carlisle, J. Gulakowski, W. Wu, C. Smith, L. Cooney, D. Blackwood, J. C. Dandrea, C. Truchot, *Energy Technol.* **2015**, *3*, 20.
[24] P.-Z. Cheng, H. Teng, *Carbon* **2003**, *41*, 2057.
[25] M. G. Fontana, *Ind. Eng. Chem.* **1955**, *47*, 81 A.
[26] J. K. Niemeier, D. P. Kjell, *Org. Process Res. Dev.* **2013**, *17*, 1580.
[27] S. Park, J. An, J. R. Potts, A. Velamakanni, S. Murali, R. S. Ruoff, *Carbon* **2011**, *49*, 3019.
[28] R. Miao, R. G. Compton, *J. Phys. Chem. Lett.* **2021**, *12*, 1601.
[29] L. F. Audrieth, P. H. Mohr, *Chem. Eng. News Archive* **1948**, *26*, 3746.
[30] A. M. Moliner, J. J. Street, *J. Environ. Qual.* **1989**, *18*, 483.
[31] W. Wu, S. Shabhag, J. Chang, A. Rutt, J. F. Whitacre, *J. Electrochem. Soc.* **2015**, *162*, A803.

Manuscript received: March 29, 2023
Revised manuscript received: May 9, 2023
Accepted manuscript online: May 19, 2023
Version of record online: June 1, 2023